ELSEVIER

Biochimica et Biophysica Acta 1368 (1998) 115–128

BIOCHIMICA ET BIOPHYSICA ACTA
BBA

Electrostatic and structural properties of complexes involving plasmid DNA and cationic lipids commonly used for gene delivery [1]

Nicolaas J. Zuidam [2], Yechezkel Barenholz *

Department of Biochemistry, The Hebrew University-Hadassah Medical School, P.O. Box 12272, Jerusalem 91120, Israel

Received 15 July 1997; accepted 31 July 1997

Abstract

The present study is aimed to characterize the interactions between plasmid DNA and cationic, large unilamellar vesicles, 110 ± 20 nm in size, composed of lipids commonly used for transfections including DOTAP/DOPE (mole ratio 1/1), DOTAP/DOPC (mole ratio 1/1), 100% DOTAP, or DC-CHOL/DOPE (mole ratio 1/1). [Abbreviations: DOTAP, *N*-(1-(2,3-dioleoyloxy)propyl)-*N*,*N*,*N*-trimethylammonium chloride; DOPE, 1,2-dioleoyl-*sn*-glycero-3-phosphatidylethanolamine; DOPC, 1,2-dioleoyl-*sn*-glycero-3-phosphatidylcholine; DC-CHOL, 3β-[*N*-(*N*′,*N*′-dimethylaminoethane)carbamoyl] cholesterol]. A novel approach of combining Gouy–Chapman calculations and fluorescence measurements of the pH at the surface of lipid assemblies by the fluorophore 4-heptadecyl-7-hydroxycoumarin showed that electrostatic parameters played a key role in the instantaneous formation of the DNA–lipid complexes upon addition of different amounts of plasmid DNA to cationic liposomes in 20 mM Hepes buffer (pH 7.4). Addition of large amounts of plasmid DNA leads to neutralization of 60% of the protonated DC-CHOL in DC-CHOL/DOPE (1/1) assemblies and 80% of the DOTAP in lipid assemblies. The characterization of these electrostatic parameters of the complexes suggests better and closer surrounding of plasmid DNA by lipids when DOPE is present. Time-dependent static light-scattering measurements monitored the formation of complexes and also showed that these complexes were highly unstable with respect to size at DNA/cationic lipid molar ratios between 0.2 and 0.8. © 1998 Elsevier Science B.V.

Keywords: Cationic liposome; 4-Heptadecyl-7-hydroxycoumarin; Surface potential; Gene delivery; Fluorescence; Static light-scattering

1. Introduction

Cationic lipid complexes have been widely used for the delivery of genes into mammalian cells and

Abbreviations: CAC, critical aggregation concentration; DC-CHOL, 3β-[*N*-(*N*′,*N*′-dimethylaminoethane)carbamoyl] cholesterol; DOPC, 1,2-dioleoyl-*sn*-glycero-3-phosphatidylcholine; DOPE, 1,2-dioleoyl-*sn*-glycero-3-phosphatidylethanolamine; DOTAP, *N*-(1-(2,3-dioleoyloxy)propyl)-*N*,*N*,*N*-trimethylammonium chloride; DOTMA, *N*-(1-(2,3-dioleyloxy)propyl)-*N*,*N*,*N*-trimethylammonium chloride; HC, 4-heptadecyl-7-hydroxycoumarin; Hepes, *N*-(2-hydroxyethyl)piperazine-*N*′-(2-ethanesulfonic acid); LUV, large unilamellar vesicles; pK_a, apparent proton binding constant, Zwittergent 3–14, *N*-tetradecyl-*N*,*N*-dimethylammonia-1-propane sulfonate

* Corresponding author. Fax: +972-2-6411663; E-mail: yb@cc.huji.ac.il

[1] A preliminary report of this study was presented at the 3rd annual conference: Artificial Self-Assembling Systems for Gene Delivery, organized by Cambridge Healthtec Institute, November 17–18, 1996, Coronado, CA.

[2] Present address: Department of Pharmaceutics, Utrecht University, P.O. Box 80.082, 3508 TB Utrecht, The Netherlands.

PII S0005-2736(97)00187-9

currently they are also being tested in several clinical trials [1–3]. The first step in the transfection process is the formation of the DNA–lipid complex. Entry of this complex into cells is probably mainly by adsorptive endocytosis [4–6] although fusion [4,5] and incorporation through membrane pores [7] cannot be ruled out. The intracellular fate of the complex will be decided by the extent of degradation in the lysosomes. In general, only a small fraction of the DNA will not be degraded by the lysosomal enzymes and will be released into the cytosol [5,6]. The last step in the transfection process is the entry of cytoplasmic DNA or DNA–lipid complex into the nucleus and the expression of the DNA. The cationic lipid complexes might play a role in each step of the transfection process. The stage in which lipid and DNA dissociate is not yet clear.

In most cases, transfection efficiency in cell cultures is dependent on the type of cells [1,8] and, for each cell type, on liposome composition and properties [1,4,9,10]. Efforts have been made to gain insight into the influences of DNA/lipid ratio [4,8,10], type of cationic carrier [1,10], lipid composition [4,10], type of liposome (size, number of lamellae [9,10]), size of DNA [7], and presence [11] or absence [11,12] of serum in the incubation medium.

The cationic lipid complexes are composed of an amphipathic mono- or polycationic carrier and a ''helper lipid''. Examples of such cationic carriers are the monocationic lipids DOTMA [11,13,14], DOTAP [15], DC-CHOL [8], and the polycationic lipid lipopoly(L-lysine) [4,12]. In most experiments all these amphipathic, cationic lipids showed optimal expression of the tested genes when mixed with the helper lipid DOPE [4,10]. The optimal mole ratio of monocationic lipid/DOPE is about 1 [10]. Replacement of DOPE by most other lipids differing in headgroup and/or fatty acyl chain composition reduces the transfection efficiency of DNA into cells [4,10]. Interestingly, more transfection activity was found when using lipopoly(L-lysine) without a helper lipid and when treated cells were scraped before transfection [12], and better delivery of a protein into cells was found in the presence of DOTMA liposomes than in the presence of DOTMA/DOPE (1/1) liposomes [16].

In spite of all these extensive efforts, it is still not clear if the influences found can be generalized or explained. Moreover, some results were contradictory. To our knowledge effects of other parameters, such as DNA structure (linear or circular), composition of incubation medium (pH, ionic strength, etc.), sequence of mixing (DNA to cationic lipids or vice versa), and incubation time before transfection, on the transfection process are not yet known. The main reasons for lack of information is that it is very hard to compare various experiments due to the large number of variable parameters and the lack of basic knowledge [17]. Therefore, currently, optimization and development of new cationic carriers for genes are performed mainly by trial and error. As stated before by others [17,18], the lack of detailed, fundamental information is severely delaying future progress.

Previously, we described electrostatic parameters and stability characteristics of cationic liposomes by use of the fluorophore 4-heptadecyl-7-hydroxycoumarin (HC) [19]. In the present study we use HC to characterize the electrostatic parameters of DNA–lipid complexes, the formation of which is the first step in the transfection process. This new approach monitored changes in the plane of interaction between plasmid DNA and lipid assemblies containing cationic lipid. Additional information about the structure of the complexes was provided by determining time-dependent changes in static light-scattering.

2. Materials and methods

2.1. Materials

An *Escherichia coli* containing the plasmid pS16-GH (4.8 kbp; for further details see [20]) was kindly given by Dr. O. Meyuhas of our department. DOTAP, DOPE, and DOPC were obtained from Avanti Polar Lipids (Alabaster, AL, USA). DC-CHOL was a generous gift of Dr. L. Huang of the Department of Pharmacology and Pharmaceutical Sciences, University of Pittsburgh, Pittsburgh, PA, USA. HC was purchased from Molecular Probes (Eugene, OR, USA). These and all other chemicals were of analytical grade. Double-distilled water was used.

2.2. DNA preparation

Plasmid pS16-GH was grown in *Escherichia coli* and isolated using a QIAGEN Mega Plasmid Kit (QIAGEN, Hilden, Germany) according to manufacturer's instructions. The final concentration of plasmid DNA in 20 mM Hepes buffer (pH 7.4) was quantified by organic phosphate determination [21]. The concentration of DNA in the present study is expressed as equivalent concentration of phosphate. Agarose gel (1%) electrophoresis showed the plasmid DNA was mainly in a supercoiled form and there was no chromosomal DNA or RNA present. UV-spectroscopy showed no presence of contamination of proteins in the several DNA batches: the ratio of absorbance at 260 nm/280 nm was about 1.8–1.9 and the absorbance at 320 nm was negligible [22].

2.3. Liposome preparation

Preparation of liposome dispersions, incorporation of HC, and measurement of liposome size distribution were performed as described in [19].

2.4. Fluorescence and static light-scattering measurements

Cationic liposomes were diluted in 3 ml of 20 mM Hepes buffer (pH 7.4) to a concentration of 4×10^{-5} M of the cationic lipid. The measurements were performed on an LS50B luminescence spectrometer (Perkin Elmer, Norwalk, CT, USA) while stirring at ambient temperature. The advantages of HC as a pH- and potential-sensitive fluorescent membrane probe are discussed in [19]. Fluorescence of HC was measured at excitation wavelengths of 330 nm (the pH-independent isosbestic point) and 380 nm using a constant emission wavelength at 450 nm (bandwidths 5 nm). An emission filter of 430 nm was used. The use of the isosbestic point enabled us to correct for differences in fluorescence intensities due to small differences in HC concentration or aggregation of the complexes. Static light-scattering of the same sample was obtained on the same spectrometer using both excitation and emission wavelength at 600 nm (bandwidths 2.5 nm). Each measurement was performed at least twice with both liposomes and plasmid DNA from different batches.

3. Results

3.1. Fluorescence of HC in DNA–lipid complexes

Appropriate amounts of plasmid DNA were added to cationic LUV containing the fluorophore HC. The amount of plasmid DNA in this study is expressed as the amount of DNA-phosphate. The change in the dissociation (or ionization) degree of HC in the lipid layers was monitored with time by measuring the value of the ratio of the excitation intensity at 380 nm to that at the isosbestic point of 330 nm while using 450 nm as the emission wavelength. As an example, the change in the ratio of the excitation intensities at 380 nm and 330 nm of HC in 8×10^{-5} M DOTAP/DOPE (1/1) liposomes upon addition of different amounts of plasmid DNA was measured continuously against time (Fig. 1). A major decrease in the ratio of the excitation intensities at 380 nm and 330 nm of HC (due to the decrease in the pH sensitive 380 nm intensity) was found immediately when plasmid DNA was added. No significant change in the absolute intensity of the fluorescence at the isosbestic point (excitation at 330 nm) was observed. The

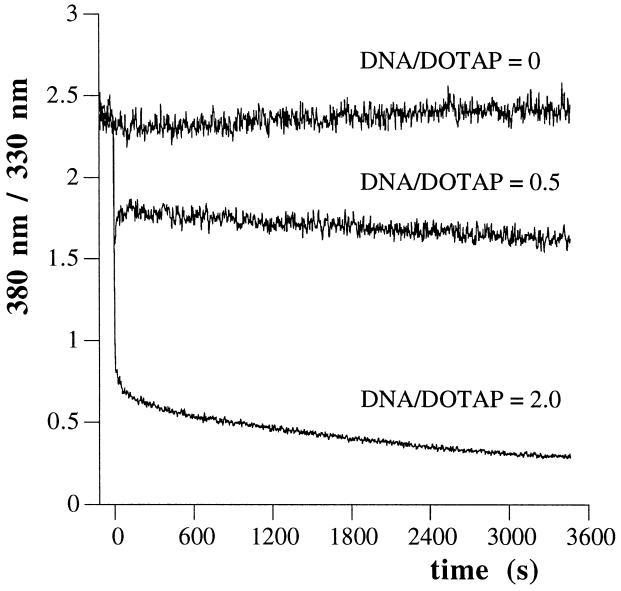

Fig. 1. Typical examples of the change in the ratio of the excitation fluorescence intensities at 380 nm and 330 nm of HC in 8×10^{-5} M DOTAP/DOPE (1/1)-LUV upon addition of plasmid DNA at time 0. The final mole ratios DNA/DOTAP are indicated in the figure.

decrease found depended on the amount of plasmid DNA. Previously [19], we also found a change in the dissociation degree of HC upon dilution of the liposomes (with or without DNA), probably due to desorption of the DOTAP from the bilayers into the bulk (CAC of DOTAP is 7×10^{-5} M). However, this process took place on a time scale of hours, while the change in the electrostatic parameters of HC in the lipid layers upon addition of plasmid DNA occurred after seconds. Therefore, we assume that the observed changes in dissociation degree of HC in the cationic bilayers measured until 15 min after addition of plasmid DNA to liposomes represent only the change in surface potential induced by the plasmid DNA.

In Fig. 2, the ratios of the fluorescence excitation intensities at 380 nm and 330 nm of HC in cationic lipid assemblies upon addition of plasmid DNA are shown as measured by excitation scans at different time intervals. Addition of plasmid DNA to the cationic liposomes caused a decrease of the dissociation degree of HC in the lipid assembly. In Fig. 2,

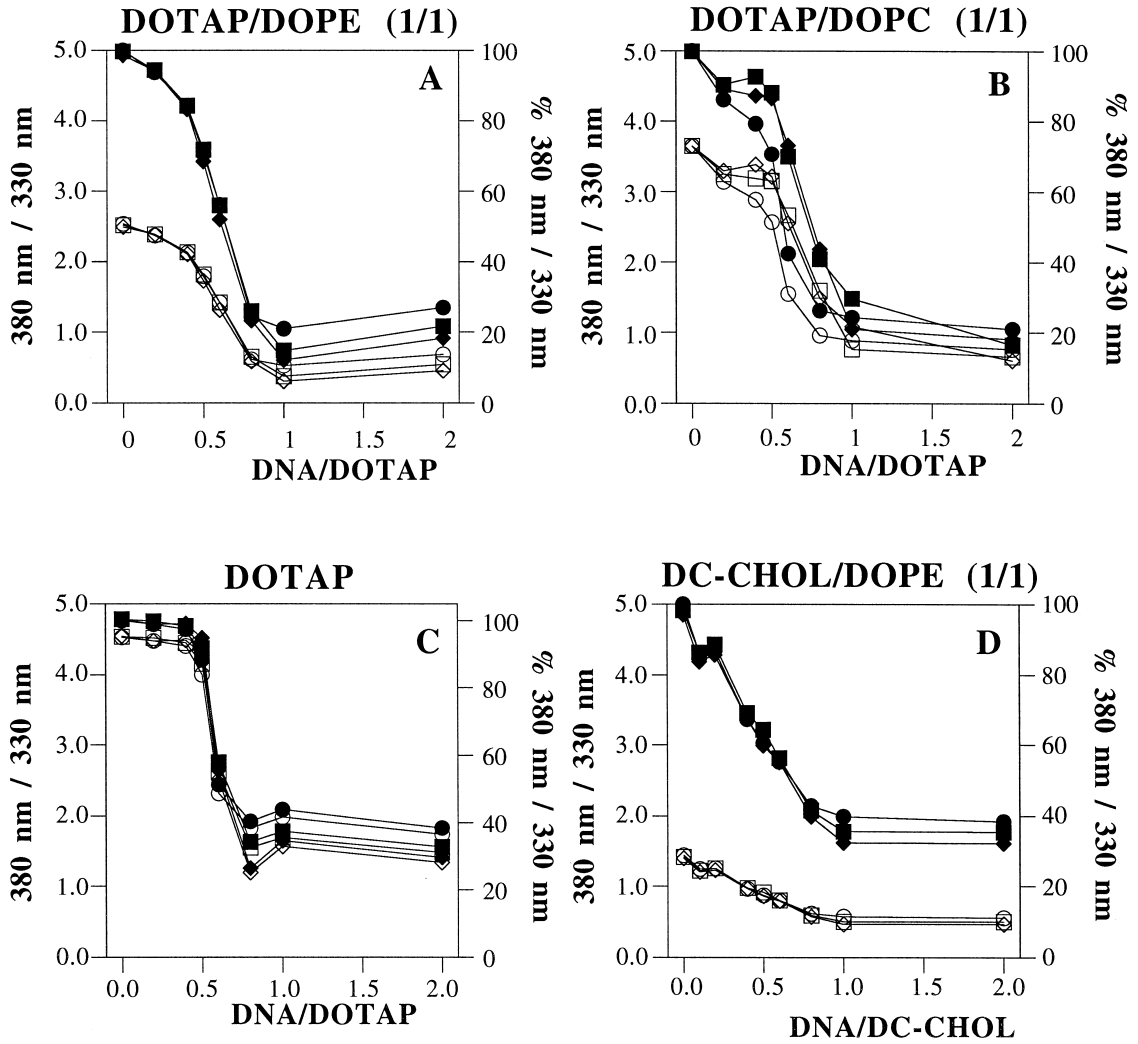

Fig. 2. Change in the ratio of the excitation fluorescence intensities at 380 and 330 nm of HC in the cationic membranes upon addition of plasmid DNA to cationic liposomes as a function of the mole ratio of DNA/cationic lipid at different time periods ($n = 2$). The compositions of the cationic liposomes were DOTAP/DOPE 1/1 (A), DOTAP/DOPC 1/1 (B), 100% DOTAP (C), and DC-CHOL/DOPE 1/1 (D). The data were measured 30 s (○), 5 min (□), and 15 min (◇) after addition of the plasmid DNA. The data are also shown as percentages of the initial values (filled symbols).

these decreases are also shown as percentages of the initial values. Both Fig. 1 and Fig. 2 show that the response time of the interaction between plasmid DNA with the cationic LUV was fast (within 10 s, probably the mixing time) and did not significantly change with time. The curve describing the decrease in dissociation degree of HC upon addition of higher amounts of plasmid DNA was almost linear when added to DC-CHOL/DOPE (1/1) liposomes (see Fig. 2(D)), but not when added to liposomes containing DOTAP (see Fig. 2(A–C)). The dissociation curve of HC in DOTAP/DOPE (1/1) against the DNA/DOTAP ratio resembles an inverted sigmoid (Fig. 2(A)). Hardly any change in dissociation degree of HC in DOTAP assemblies lacking DOPE could be observed upon addition of relatively low amounts of plasmid DNA (DNA/DOTAP $\leq$ 0.5; see Fig. 2(C)). At a DNA/DOTAP ratio of 0.2, addition of plasmid DNA changed the dissociation degree of HC in DOTAP/DOPC (1/1) assemblies, but no further change occurred when higher amounts of plasmid DNA were added until a ratio of DNA/DOTAP of about 0.5 was reached (Fig. 2(B)). As in the case of the 100% DOTAP assemblies (Fig. 2(C)), only rela-

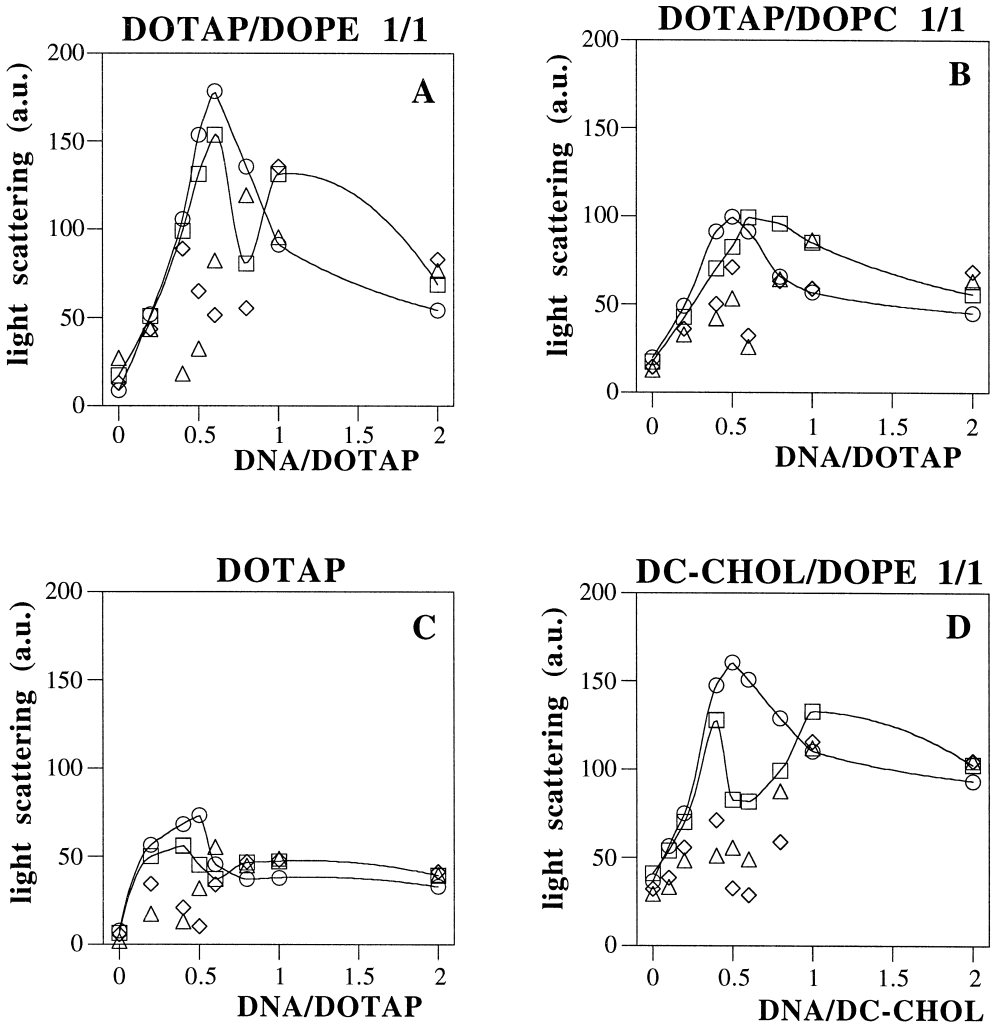

Fig. 3. Static light-scattering at 600 nm of DNA/lipid complexes upon addition of plasmid to cationic liposomes as a function of the mole ratio of DNA/cationic lipid and at different time periods ($n = 2$). The compositions of the cationic liposomes were DOTAP/DOPE 1/1 (A), DOTAP/DOPC 1/1 (B), 100% DOTAP (C), and DC-CHOL/DOPE 1/1 (D). The data were measured at 30 s (○), 15 min (□), 3 h (◇), and 24 h (△) after addition of the plasmid DNA. Lines were drawn through the points of 30 s and 15 min. Data points measured at the other time periods not on these lines indicate aggregation of the complexes with time.

tively high amounts of plasmid DNA were able to further change the dissociation degree of HC in the DOTAP/DOPC (1/1) assemblies. When using DOTAP/DOPC (1/1) LUV, the dissociation degrees of HC in the DNA–lipid complexes at DNA/DOTAP ratios between 0.2 and 0.8 were somewhat smaller 30 s after mixing than at other time points. Simultaneously, large changes in the static light-scattering with time (see Fig. 3(B) and text below) and, finally, flocculation (by eye) were observed. This precipitation process might be the cause of the ''noise'' in the fluorescence intensity measurements. The maximal change in the dissociation degree of HC in 100% DOTAP assemblies was reached at a DNA/DOTAP mole ratio of 0.8 and in all other lipid assemblies at a DNA/cationic lipid ratio of 1.0. This plateau was reached at a level of 20%–30% of the initial value for the assemblies containing DOTAP and at $\sim$40% of the initial value in the case of DC-CHOL/DOPE (1/1) assemblies. Addition of DNA to cationic liposomes never resulted in HC reaching the level of 100% protonation, although the full scale of protonation from 0% to 100% could be achieved by changing the pH of the medium (see Fig. 1 in Ref. [19]).

3.2. Static light-scattering of DNA–lipid complexes

Time-dependent changes in static light-scattering (see Fig. 3) were measured in parallel to the fluorescence measurements shown in Fig. 2. A solution of 8×10^{-5} M plasmid DNA in the absence of cationic liposomes (≤ 4 a.u.) or a solution of only liposomes (8 and 20 a.u. for 4×10^{-5} M DOTAP and 8×10^{-5} M DOTAP/helper lipid (1/1) liposomes and 30 a.u. for 8×10^{-5} M DC-CHOL/DOPE (1/1) liposomes) hardly scattered. Increases in static light-scattering to almost their maximal values were found immediately (< 30 s) upon addition of the plasmid DNA to all cationic liposomes studied. Concerning the effect of ratio of DNA to cationic lipid, the maximal static light-scattering upon addition of plasmid DNA to the cationic liposomes was obtained when the mole ratio of DNA/cationic lipid was 0.6. These maximum values were dependent on the lipid composition: DOTAP/DOPE (1/1) $\approx$ DC-CHOL/DOPE (1/1) > DOTAP/DOPC (1/1) > 100% DOTAP. At higher DNA/cationic lipid ratios the instantaneous increases in static light-scattering of the DNA/lipid complexes were smaller than at lower ratios. The time-dependent decrease in static light-scattering of the DNA–lipid complexes demonstrates that these complexes were unstable, especially at DNA/cationic lipid ratios between 0.2 and 0.8. The decreases in the light-scattering of the DNA–DOTAP/DOPE (1/1) and DNA–DC-CHOL/DOPE (1/1) complexes with time were most pronounced at DNA/cationic lipid molar ratios between 0.4 and 0.8. The reduction in the light-scattering of the DNA–DOTAP/DOPC (1/1) and DNA–DOTAP complexes was most pronounced at DNA/DOTAP molar ratios between 0.4 and 0.6 and between 0.2 and 0.6, respectively. The increases in static light-scattering of DNA–lipid complexes at charge ratios > 1.0 were smaller and much less affected by incubation time. The decreases in static light-scattering monitored aggregation and precipitation of the complexes with time (then white flocculates could be clearly seen by eye at the bottom of the cuvette).

4. Discussion and conclusions

The fluorescent probe HC incorporated in liposomes is located in the lipid bilayer with its long-chain tail parallel to the lipid acyl chains and its pH- and electrical surface potential-sensitive fluorophore present at the water/lipid interface. It has the unique property that its fluorescence lifetime is unaffected by temperature or by the physical state of the lipids; also, its fluorescence is evenly distributed in the membrane plane, irrespective of lateral phase separation [24,25]. Thus, changes in the dissociation degree of HC in the lipid layers upon addition of plasmid DNA to liposomes (see Fig. 1) will reflect mainly changes in the electrostatic properties of the water/lipid interface. Encouraged by the good agreement between the experimental data of $pH_{surface}$ and Ψ_0 of cationic liposomes obtained by fluorescent measurements of HC and by Gouy–Chapman calculations, shown in the preceding article [19], we calculated the percent change of positively charged lipids upon addition of plasmid DNA by combining the fluorescence measurements of HC in the complexes with Gouy–Chapman calculations. The details of these calculations are shown in the appendix of this article and the results are presented in Fig. 4. Fig. 1

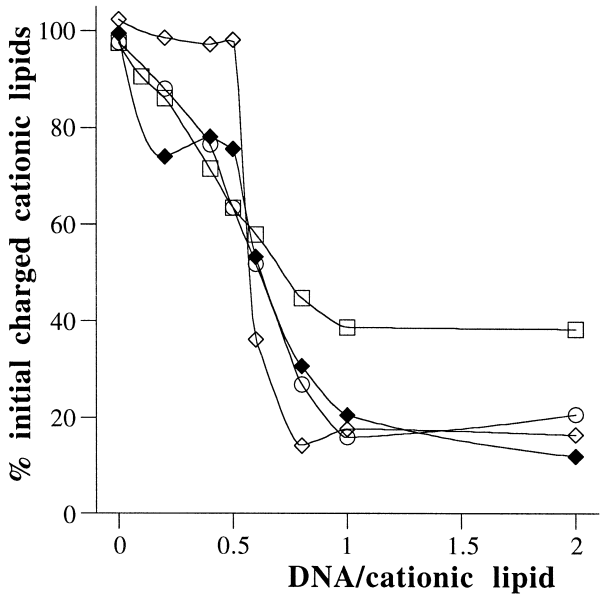

Fig. 4. Percentage of charged cationic lipids in the lipid assemblies upon addition of plasmid DNA to cationic liposomes as a function of the mole ratio of DNA/cationic lipid at 15 min ($n = 2$). The data were calculated from the measurements shown in Fig. 2. See appendix and text for further details. The compositions of the cationic liposomes were DOTAP/DOPE 1/1 (○), DOTAP/DOPC 1/1 (◆), 100% DOTAP (◇), and DC-CHOL/DOPE 1/1 (□).

and Fig. 2 showed that after the first instantaneous change, further changes were small and occurred over much longer time scales (many hours). Therefore, in Fig. 4 we describe the change in percent charged cationic lipids measured 15 min after addition of plasmid DNA to cationic liposomes. The % charged cationic lipid at pH_{bulk} of 7.4 was set at 100% in Fig. 4, the absolute values are described in [19]. It is striking that the curves of the percent charged lipids shown in Fig. 5 are almost identical to the curves of the percent change in the dissociation degree shown in Fig. 2. This can be explained by Fig. 5, which shows that up to a σ of 0.125 C/m^2 an almost linear relationship exists between σ and the dissociation degree of HC in cationic liposomes at pH_{bulk} 7.4. The validity of this theoretical relationship is supported by experimental data on the dissociation degree of HC in cationic liposomes at pH_{bulk} 7.4 obtained previously [19]. We would like to stress here that large changes in variable parameters of the Gouy–Chapman calculations did not significantly affect the outcome of the calculations of the percent charged lipids, and that confocal fluorescence microscopy showed a homogeneous distribution of the fluorescence of HC in large DNA–lipid complexes (data not shown).

In previous studies, the apparent proton binding constant (pK_a) of HC was always determined to calculate the surface potential of liposomal bilayers [26–28]. The approach described in the present paper makes it possible to follow the kinetics of changes of the electrostatic interactions with time, unlike determining the pK_a of HC. We assume that this new approach can also be applied to study the electrostatic interactions between liposomes and proteins or between liposomes and ions. It might also be applied to study interactions with other lipid assemblies such as emulsions or micelles. A limitation of this method is that the electrostatic interactions can only be determined in the pH-range in which the fluorophore is responsive to the added agent, unlike zeta potential

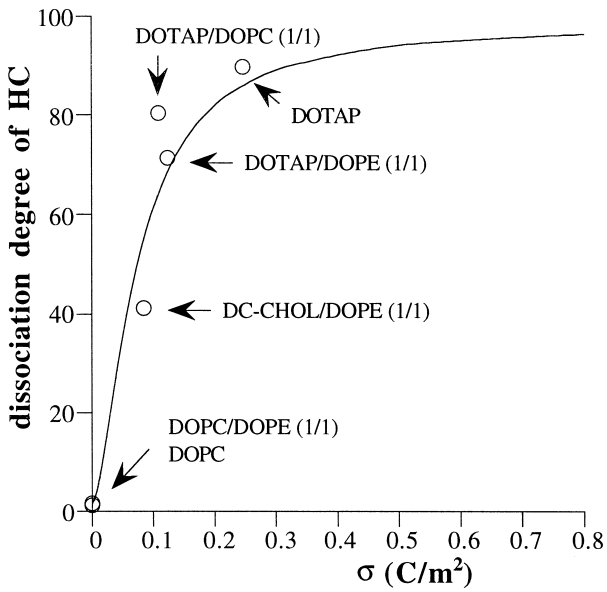

Fig. 5. Theoretical relationship between the surface charge density (σ) of LUV and the dissociation degree of HC in these bilayers at pH_{bulk} 7.4. The relationship was obtained by calculating the $pH_{surface}$ of cationic liposomes according to Gouy–Chapman calculations (Eqs. (4)–(6) of [19]) and by calculating the dissociation degree using the curve-fit of the dissociation degree of HC in DOPC-liposomes according to Eq. (1) of [19]. Also shown are the experimental data of liposomes at pH_{bulk} 7.4 obtained from Fig. 1(B) of [19].

measurements. However, zeta potential measurements (and size measurements) by dynamic light-scattering may be misleading as they don't obey some of the basic rules of reliable application of photon correlation spectroscopy for motion and size determination [21,46]: (a) It was demonstrated that complexes may have hindered motions [30]. (b) The complexes are neither spherical nor homogeneous in size, shape, and probably composition [6,23,29–32]. (c) Moreover, free plasmid DNA and possibly DNA in some of the complexes have a significant rotational component in addition to the lateral component (used to calculate size by means of the diffusion coefficient). This rotational component is not taken into consideration by most commercial photon correlation spectrometers as their analysis is not using a forced homogeneous model [33]. Other advantages of using the fluorophore HC over zeta potential measurements are that this fluorophore provides information on the lipid headgroup region [24–28,35] and not at the plane of shear (like the zeta potential [34]); and that it monitors the electrical potential at all water/lipid interfaces where HC is present and not only at the external surface (as was recently shown in [29]). Although zeta potential measurements indicate the charge ratio of DNA to cationic lipids at which neutralization at the plane of shear of the external surface of the complex occurred [34], they are not sensitive enough to give the fine details about the titration of cationic lipids by DNA (compare Fig. 3 in [29] with Fig. 2 of the present study). Therefore, our measurements using HC are complementary to zeta potential measurements.

The following characteristics of plasmid DNA–lipid complexes and of the interactions between plasmid DNA and lipid assemblies were observed:

(a) *Close and instantaneous contact*: Addition of plasmid DNA to cationic liposomes changed the dissociation degree of HC in the lipid assembly instantaneously and this remained constant and unalterated (in all of DNA/cationic lipid ratios tested) (see Fig. 1 and Fig. 2). Based on previous experiments with HC in micelles composed of the zwitterionic detergent Zwittergent 3–14 ([35], see below for more details), we conclude that the distance between the plasmid DNA and the cationic bilayers must have been smaller than 6Å. The very close contact between the plasmid DNA and the cationic bilayers was also demonstrated by us recently [36,37], showing that DNA and cationic membranes approached each other so close that the fluorophore 1-(4-trimethylammoniumphenyl)-6-phenylhexa-1,3,5-triene (TMA-DPH) could monitor changes in the hydration of the lipid layer. At DNA/cationic lipid ratios < 0.6, an increase in the exposure of the TMA-DPH in the membranes to water was found, while a dehydration was observed at DNA/cationic lipid ratios ≥ 1.

(b) *Neutralization of the positive lipid charges*: Gouy–Chapman calculation presented in Fig. 5 shows that the helper lipid present in 1/1 mole ratio with the cationic lipid has a large effect on the surface positive charge density. At the surface of 100% DOTAP LUV the charge density is higher than for DOTAP/DOPE (1/1) LUV (compare 0.27 and $0.13\,C/m^2$, respectively). Examining the negative charge density on the B helix, DNA gives a value of $\sim 0.15\,C/m^2$ (based on a helix step of 0.34 nm per bp = 0.17 nm per DNA-phosphate, and the helix being a cylinder with a surface area of $1.07^{-18}\,m^2$ [3,45]). Thus the positive charge density of LUV having 50 mol% zwitterionic lipids (DOPC or DOPE) matches better than 100% DOTAP LUV the negative charge distribution of B-helix DNA. The changes in the dissociation degree of HC indicate that the cationic lipids were indeed neutralized by plasmid DNA (Fig. 5). Although many times suggested, this is the first time, to our knowledge, that neutralization of cationic lipids upon addition of plasmid DNA has been demonstrated. The neutralization requires release of counterions associated with the lipids and the DNA surfaces into the bulk phase. The dissociation degree of HC in the cationic lipid assemblies did not reach its minimum level of about 0 (see [19]) upon addition of an excess amount of negatively charged plasmid DNA (see Fig. 2). This indicates that not all positive charges of the cationic lipids are reached and/or fully neutralized by the negatively charged phosphate groups of plasmid DNA (see Fig. 4). Another possibility might be that the location of the fluorophore HC was so close to the cationic lipid that it sensed more of the positive charge of the cationic lipid than of the negative charge of the DNA. Such a phenomenon was found before in micelles of the zwitter-ionic detergent Zwittergent 3–14, in which the positively charged quaternary amine in the water/lipid interface is spaced three carbons and a

sulfur apart from the negatively charged oxygen attached to the sulfur (about 6Å) [35].

The good agreement between the experimental data of $pH_{surface}$ and Ψ_0 of cationic liposomes obtained by fluorescent measurements of HC and by Gouy–Chapman calculations shown in [19] indicates that there is no specific interaction between HC and the cationic lipids (otherwise, the measured pK_a should have been different from the theoretical pK_a, as was the case with Zwittergent 3–14 in [35]). Our interpretation of the data might be negated by possible changes in the dielectric constant of the environment of the fluorophore due to the DNA–lipid interaction. To test this, first the sensitivity of the fluorescence intensity at the isosbestic wavelength (330 nm excitation) to the dielectric constant was demonstrated: (a) By the large differences in the fluorescence intensity of 2×10^{-7} M HC in Triton X-100 micelles (1 mM Triton) and in liposomes of the compositions described in Fig. 2 (65 a.u for Triton X-100 micelles vs. 180 a.u, for liposomes (irrespective of composition).

(b) The fluorescence intensity was strongly affected by the dioxane/water ratio. In mixtures of these two solvents giving dielectric constants of 51, 33, 17, and 10, fluorescence intensities of 148, 245, 74, and 33 a.u., respectively, were recorded. Thus, changes in the dielectric constant of the HC environment can be easily determined by the changes in the fluorescence intensity resulting from the excitation at the pH-insensitive isosbestic wavelength (330 nm). Such changes did not occur upon the interaction of DNA with the cationic LUV. Therefore, the changes in the dissociation degree of HC upon the interactions of DNA and the liposomes most likely reflects only the changes in the charge density of the surface of the lipid assemblies. The maximal amount of neutralized lipids was dependent on the type of cationic lipid: DOTAP could be maximally neutralized ~ 80% (independent of the helper lipid) and DC-CHOL in DC-CHOL/DOPE (1/1) assemblies could be maximally neutralized ~ 60% by an excess of plasmid DNA. The two cationic lipids differ both in polar headgroup and in lipophilic region. In the previous paper [19] we found that the tertiary amine of DC-CHOL in DC-CHOL/DOPE (1/1) liposomes is only 50% charged at pH 7.4, in contrast to the 100% of DOTAP quaternary amine. The different protonations of these cationic lipids might result in a different distance between the polar headgroup and the phosphate group of plasmid DNA. It is likely that dissociation of the lipids from the DNA (which is necessary for transfection [6]) will require less energy when lipid assemblies containing DC-CHOL are used than when the lipid assemblies contain fully charged lipids.

In the present study, we also found that the maximal percent neutralization of all cationic bilayers upon addition of increasing amounts of plasmid DNA was reached at about the ratio of DNA/cationic lipid of 1.0 (see Fig. 4). Only a key role for electrostatic parameters in the formation of DNA–lipid complexes can explain why an equal amount of plasmid DNA is necessary to neutralize DOTAP/DOPE (1/1) assemblies or 100% DOTAP assemblies. Covering of the strands of DNA by lipids will occur as a result of this interaction, but apparently the molecular dimensions of the cationic lipids are not a critical factor in the coverage at a DNA/cationic lipid charge ratio ≥ 1.0 [2,29]. The critical DNA/cationic lipid ratio of 1.0 has been observed before by others. Gershon et al. [32] found that above the DNA/cationic lipid mole ratio of about 1.0, two processes occurred: DNA-induced intervesicular lipid mixing, which was interpreted as vesicle fusion, and liposome-induced DNA collapse. They also found that only below the DNA/cationic charge ratio of about 1.1, ethidium bromide could not stain, and DNAse could not cleave, the DNA. Eastmann et al. [29] demonstrated that a charge ratio of 1.0 is required to bind all the DNA in a titration of DNA by cationic liposomes.

Further support for the dominant role of lowering the electrostatic free energy of the system by the charge neutralization in the process of DNA–lipid complex formation is given by the results found that DNA and DOPC/DOPE (1/1) liposomes did not interact with each other, as shown here, and by the lack of changes in the fluorescence intensity of bilayer-incorporated TMA-DPH and no changes in light-scattering [36,37]. Increase in the exposure of TMA-DPH in DOTAP/DOPE (1/1) to water upon interaction of DNA with the lipids was suggested by quenching of the fluorescence at low (≤ 0.6) DNA/cationic lipid charge ratio, while at a charge ratio ≥ 1.0, reduction in the fluorophore exposure to water led to dequenching (increase in the fluorescence intensity).

(c) *Role of the helper lipid*: Fig. 4 also shows that the neutralization of the cationic lipids in DOTAP/DOPC (1/1) or 100% DOTAP assemblies did not increase linearly with increasing amount of plasmid DNA, in contrast to DOTAP/DOPE (1/1) assemblies. It was striking that for LUV of 100% DOTAP up to a DNA/DOTAP ratio of ≤ 0.5, the DOTAP molecules did not come in such close contact with plasmid DNA that they could be monitored through HC fluorescence intensity (Fig. 2(C) and Fig. 4). This indicates that the distance should be larger than the calculated Debye length of 0.74 nm [19]). DOTAP/DOPC (1/1) assemblies at a DNA/DOTAP ratio of 0.2 are partially neutralized by plasmid DNA. However, most of the neutralization occurred only when higher amounts of plasmid DNA were added (Fig. 2(B)), and the neutralization was not as continuous as with the DOTAP/DOPE 1/1 system (Fig. 2(A)). However complex formation in all the above systems was demonstrated by light and electron microscopy (data not shown, and [36]) and from the kinetics of changes in static light-scattering upon addition of plasmid DNA to cationic liposomes. The latter is demonstrated in Fig. 3, which shows instantaneous increase in static light-scattering of these samples followed by aggregation of complexes (as monitored by the decreases in static light-scattering). Aggregation hardly affected the level of the dissociation degree of HC in these complexes (although the fluorescence intensity of HC decreased). All the above suggests that the fluorescence of HC monitors short distance DNA–lipid interaction constituting the microstructure of the complexes, while the static light-scattering monitors its macrostructure (state of aggregation). The difference between the electrostatics and the macrostructure of the complex was also demonstrated recently by Eastman et al. [29] using zeta potential as a measure for the electrostatics and dextran density gradients for the macrostructure. The ratio of DNA to cationic lipid at which neutralization of the lipid by the DNA starts to be significant (threshold of electrostatic neutralization) is affected by the LUV lipid composition. For a system of DOTAP alone the threshold charge ratio occurs at a DNA to cationic lipid charge ratio of 0.5, while for DOTAP/DOPE (1/1) LUV there is no threshold, and neutralization is continuous (Fig. 4). A few factors may be involved in this difference: (a) a salt bridge between the phosphate group of DOPE and the quaternary amine of DOTAP (Fig. 4 in [19]), which forces the primary amine of DOPE to assume a vertical conformation with respect to the bilayer plane, thereby being in closer contact with the DNA negatively charged phosphates; (b) the facilitation of the removal of cationic lipid-associated counterion; (c) the dehydrating effect of the helper lipids (such as DOPE). All these will reduce the distance between the DNA and the lipid surface. For DOTAP alone, the fact that the surface is more positively charged and more hydrated, [19,36,37] makes counterions bind more strongly than in DOTAP/DOPE LUV, and therefore the counterion release requires more DNA, which explains the neutralization DNA threshold. That is, the helper lipid may facilitate the close contact and negative curvature (when needed) through its effect on the balance between the electrostatic and bending energy contributions in the surrounding of the plasmid DNA by the lipid molecules. Based on the above considerations, it is expected that the overall effect on DNA/cationic lipid neutralization threshold would be in the order: DC-CHOL/DOPE (1/1) $\approx$ DOTAP/DOPE (1/1) > DOTAP/DOPC (1/1) > DOTAP, as described in Fig. 4. The same suggestion has been made before by Gustaffson et al. [31] using cryo transmission electron microscopy. We found additional proof for differences between DNA–DOTAP/DOPE (1/1) and DNA–DOTAP complexes by using circular dichroism: while liposomes of both lipid compositions induced DNA condensation at the level of the secondary structure (the B-helix became more overwound), only DOTAP/DOPE (1/1) lipids induced additional changes in the tertiary structure of the DNA, i.e., the appearance of ψ–DNA, which is an indication of relatively close proximity of parallel helices [37]. This finding also suggests closer contact between DNA and DOTAP/DOPE (1/1) assemblies than between DNA and 100% DOTAP assemblies. That lipid assemblies containing DOPE are better able to surround the strands of plasmid DNA has been suggested before [2,23], although the present study provides direct evidence for this hypothesis. The greater ability of lipid assemblies containing DOPE to surround DNA also corresponds well with the finding that DOPE monolayers have a large tendency to curl [38,39]. As stated in the introduction, the presence of

DOPE in cationic liposomes facilitates the transfection process [4,10], but its role is not clearly understood. It may affect one or more steps in the transfection process (such as complex formation, endocytosis of the DNA–lipid complex, and destabilization of the endosomal membrane by fusion).

(d) *Structure of the DNA–lipid complexes*: Immediately after preparation, the static light-scattering of the DNA–lipid complexes was maximal when the mole ratio DNA/cationic lipid was between 0.6 and 0.8 (Fig. 3). This suggests the formation of larger structures at these DNA/cationic lipid ratios and smaller structures at the other ratios used. Felgner et al. [2] and Sorgi and Huang [40] found similar results upon dynamic light-scattering measurements of DNA–DMRIE/DOPE (1/1) and DNA–DC-CHOL/DOPE (3/2) complexes (their maximal sizes were about 1–2 μm). Our electron and light microscopy data [36] showed larger structures heterogeneous in size (0.3–3.0 μm) and shape when plasmid DNA was added to DOTAP/DOPE (1/1) liposomes at a DNA/DOTAP charge ratio of 0.5 rather than 2.0 (data not shown), in agreement with previous reports [6,23,29–32]. The large sizes of the complexes at the relatively low DNA/cationic lipid charge ratio of 0.5, when combined with simple calculation, suggest that each DNA–lipid complex contained several plasmids. Fluorescence and freeze-fracture electron microscopy [36] indicate that each of the large (μm range) complexes formed at DNA/cationic lipid charge ratio of 0.5 is actually a cluster of closely packed particles (which may be partially fused), as was observed before by Sternberg for DNA/(DC-CHOL/DOPE) in excess of lipids (Fig. 1 and Fig. 2 in [23]).

The static light-scattering data also showed that the size of DNA–lipid complexes was very unstable with time at DNA/cationic lipid ratios of 0.4–0.8. In this range, aggregates keep increasing in size with time, unlike the complexes formed at higher DNA/cationic lipid ratios. Recent studies by Hirsch-Lerner and Barenholz [36,37] suggest that defects in the lipid assemblies due to lateral phase separation induced by the DNA in excess cationic lipids might be the cause of the observed aggregation. The instability of the complexes might influence the transfection efficiency and might explain much of its poor reproducibility.

Maximal percentages of cationic lipids which were neutralized upon addition of plasmid DNA exceed 50% (80% in DOTAP-based systems and 60% for DC-CHOL/DOPE (1/1)-based complexes). This suggests that most of the cationic lipid molecules are interacting with the DNA already at $DNA^-/lipid^+$ charge ratio = 1.0 (Fig. 4). The exact level of maximal neutralization may reflect the degree of complex polymorphism. In two forms of the complexes, the hexagonal array composed of a bundle of DNA plasmids, each covered by a monolayer of cationic lipids [2] (referred to as ''honeycomb'' structure [45]) and the multilamellar array in which both monolayers of each lipid bilayer interact with the plasmid DNA [30,31,42], maximal neutralization should be > 50%. Maximal neutralization of the cationic lipids for the honeycomb form should be higher than for the multilamellar form since in the honeycomb form all the cationic lipids can interact with the plasmid phosphates. For the multilamellar form, 100% neutralization will require very close proximity between the DNA helices, which is improbable due to electrostatic repulsion, unless the DNA induces the lipids to bend and form grooves in which the DNA is placed. Therefore in the multilamellar form maximal neutralization will be between 50%–100%. In the third form of the complex, in which a cylinder of one lipid bilayer surrounds a supercoiled plasmid DNA (''spaghetti'' form [23]), the level of maximal neutralization should be ≤ 50% depending on the distribution of cationic lipids between the inner and outer layers of the spaghetti bilayer. Therefore it is expected that the more enriched is the system with the spaghetti form, the closer to 50% will be the maximal neutralization. Indeed, the complexes of DC-CHOL/DOPE with DNA have a high occurrence of the spaghetti form, which may in part explain their lower level of maximal neutralization. Recent studies on monocationic lipid DNA complexes based on cryotransmission EM [31], X-ray scattering [30], and a combination of cryotransmission EM and small-angle X-ray scattering [41], suggest that at an excess of cationic lipid, the complex is indeed multilamellar, characterized by a short-range lamellar symmetry due to the entrapment of DNA between fluid lipid lamellae. Freeze-fracture electron microscopy (23) supports the dominance of the lamellar phase.

Recent theoretical calculations of Dan [42] based on a simple model of lipid assembly [43,44] support

higher stability of the multilamellar structure, while calculations performed by May and Ben-Shaul [45], based on the balance between the energetic gain from lowering the electrostatic free energy due to neutralization and the energetic loss due to adaptation of the lipids to the complex geometry (bending energy), indicate that the spaghetti form is thermodynamically feasible although it is less stable than the honeycomb or the multilamellar forms. The preference between the three complex forms described above has still to be determined and may be dependent on the exact lipid composition, on the DNA/cationic lipid charge ratio, and on the medium. This however, does not answer the controversial question whether the multilamellar complex form is encapsulated by a lipid bilayer [1] or not [29]. A study which correlates the transfection efficiency with the electrostatics and macrostructure of cationic-lipid/DNA-based complexes is now underway in order to evaluate the contribution of each of these two variables

Acknowledgements

This work was supported in part by Israel Science Foundation grant 494/96 to Y. B. and by the Valazzi-Pikovsky Fellowship Fund to N.J. Z. We would like to thank the following colleagues: Dr. O. Meyuhas of our department and Dr. L. Huang of the Department of Pharmacology and Pharmaceutical Sciences, University of Pittsburgh, Pittsburgh, PA, USA, for their gifts of the *Escherichia coli* containing the plasmid pS16-GH and the DC-CHOL, respectively; Dr. E. Rahamim of the Interdepartmental Equipment Unit Electron Microscopy Laboratory of our medical school for performing negative staining/rotary shadowing electron microscopy; Dr. N. Dan of the Department of Chemical Engineering, University of Delaware, Newark, Delaware, and Drs. S. May and A. Ben-Shaul of the Department of Physical Chemistry, The Hebrew University, Jerusalem, Israel for discussing with us theoretical aspects of DNA–cationic lipid interaction and showing us their manuscripts prior to publication ([45] and [42] respectively). Finally, we thank Mr. S. Geller for his help in editing the manuscript.

Appendix A. Calculation of % charged lipids in the DNA–lipid complexes

The curve of HC in DOPC-liposomes (shown in [19]) was fitted to a modified Henderson–Hasselbach equation:

$$\mathrm{pH}_{\mathrm{bulk}} = \mathrm{p}K_{\mathrm{a}} + A\log\left(\frac{D - D_{\min}}{D_{\max} - D}\right) + \log\left(\frac{I_{\mathrm{a}}}{I_{\mathrm{b}}}\right) \qquad (1)$$

where the constant A is ideally 1 since the protonation of HC is a one-to-one event (here 1.26); $\mathrm{p}K_{\mathrm{a}}$ is the apparent proton binding constant of HC (here 10.5); D is the dissociation degree; $D_{\min}$ and $D_{\max}$ are the minimum and maximum values of D, respectively (here 1.0 and 98.7); $I_{\mathrm{a}}/I_{\mathrm{b}}$ is the ratio of the fluorescence intensity of the pH-independent isosbestic point of HC (excitation at 330 nm) and of the unprotonated charged HC (excitation at 380 nm). $\mathrm{Log}(I_{\mathrm{a}}/I_{\mathrm{b}})$ is 0 at an ideal isosbestic point; here -0.1). By estimating the dissociation degree of HC in lipid bilayers and by using Eq. (1), the average $\mathrm{pH}_{\mathrm{surface}}$ of these lipid bilayers can be estimated. This method was used to estimate the change in the average $\mathrm{pH}_{\mathrm{surface}}$ of the cationic bilayers ($\Delta\mathrm{pH}_{\mathrm{surface}}$) upon addition of the plasmid DNA. The value of $\Delta\mathrm{pH}_{\mathrm{surface}}$ upon addition of plasmid DNA was used to calculate the change in surface potential, $\Delta\psi_0$, using the Boltzmann equation for a given potential:

$$\Delta\psi_0 = \frac{\Delta\mathrm{pH}_{\mathrm{surface}} kT \ln 10}{e} \qquad (2)$$

where k is the Boltzmann constant (1.38×10^{-23} $\mathrm{J \cdot K^{-1}}$), T is the absolute temperature (here 295 K), and e is the electron charge (1.6×10^{-19} C). The initial ψ_0 of the cationic bilayers in the absence of plasmid DNA was calculated by Gouy–Chapman approximation:

$$\psi_0 = \left(\frac{2\,kT}{ze}\right)\sinh^{-1}\left(\frac{ze\,\sigma\lambda}{2\,\varepsilon_0\varepsilon_{\mathrm{r}}\,kT}\right) \qquad (3)$$

where z is the valency of the counterions (in the present study, 1), σ is the surface charge density ($\mathrm{C \cdot m^{-2}}$), λ is the Debye screening length (m), ε_0 is the relative permittivity of free space (8.85×10^{-12} $\mathrm{C^2 \cdot J^{-1} \cdot m^{-1}}$), and ε_{r} is the dielectric constant at

the location of the fluorophore moiety, with a value of 8 (see [19] for its estimation). The values of σ were calculated taking a molecular surface area of 0.82 nm^2 for DOPC, 0.65 nm^2 for DOPE, 0.30 nm^2 for DC-CHOL, and 0.65 nm^2 for DOTAP. λ is given by:

$$\lambda = \sqrt{\frac{\varepsilon_0 \varepsilon_r kT}{N e^2 \sum c_i z_i}} \quad (4)$$

where N is the Avogadro constant and c_i is the concentration of all individual ions (here 0.017 mol · m^{-3}). In the present study, a value of 0.74 nm for λ was calculated. The values of ψ_0 of the cationic bilayers in the absence of plasmid DNA are published in Ref. [19]. The ψ_0 of the cationic bilayers in the presence of plasmid DNA was obtained by adding together its initial value obtained with Eq. (3) and the $\Delta\psi_0$ obtained by Eq. (2). Finally, the value of σ in the presence of plasmid DNA was estimated using a converted form of Eq. (3):

$$\sigma = \left(\frac{2\ \varepsilon_0 \varepsilon_r\ kT}{z e\ \lambda}\right) \sinh\left(\frac{\psi_0\ ze}{2\ kT}\right) \quad (5)$$

Then, the change in the surface charge density, $\Delta\sigma$, and thus the percent of charged lipids, can be calculated. For further information about these calculations and assumptions made, please see Ref. [19].

References

[1] J.S. Remy, C. Silin, J.P. Behr, in: J.R.S. Phillippol, F. Schuber (Eds.), Liposomes as Tools in Basic Research and Industry, CRC Press, Boca Raton, FL, 1995, pp. 159–170.

[2] P.L. Felgner, Y.J. Tsai, J.H. Felgner, in: D.D. Lasic, Y. Barenholz (Eds.), Handbook of Nonmedical Applications of Liposomes, vol. 4, CRC Press, Boca Raton, FL, 1996, pp. 43–56.

[3] D.D. Lasic, Liposomes in Gene Delivery, CRC Press, Boca Raton, FL, 1997.

[4] X. Zhou, L. Huang, Biochim. Biophys. Acta 1189 (1994) 195–200.

[5] K. Goyal, L. Huang, J. Liposome Res. 5 (1995) 49–60.

[6] J. Zabner, A.J. Fasbender, T. Moninger, K.A. Poellinger, M. Welsh, J. Biol. Chem. 270 (1995) 18997–19007.

[7] I. Van der Woude, H.W. Visser, M.B.A. Ter Beest, A. Wagenaar, M.H.J. Ruiters, J.B.N.F. Engberts, D. Hoekstra, Biochim. Biophys. Acta 1240 (1995) 34–40.

[8] X. Gao, L. Huang, Biochem. Biophys. Res. Commun. 179 (1991) 280–285.

[9] K. Yagi, H. Noda, M. Kurono, N. Ohishi, Biochem. Biophys. Res. Commun. 196 (1993) 1042–1048.

[10] J.H. Felgner, R. Kumar, S.H. Sridhar, C.J. Wheeler, Y.J. Tsai, R. Border, P. Ramsey, M. Martin, P.L. Felgner, J. Biol. Chem. 269 (1994) 2550–2561.

[11] E. Brunette, R. Stribling, R. Debs, Nucleic Acids Res. 20 (1992) 115.

[12] X. Zhou, A.L. Klibanov, L. Huang, Biochim. Biophys. Acta 1065 (1991) 8–14.

[13] G.M. Ringold, M. Danielsen, Proc. Natl. Acad. Sci. U.S.A. 84 (1987) 7413–7417.

[14] P.L. Felgner, M. Holm, Focus 11 (1989) 21–25.

[15] R. Leventis, J.R. Silvius, Biochim. Biophys. Acta 1023 (1990) 124–132.

[16] R.J. Debs, L.P. Freedman, S. Edmunds, K.L. Gaensler, N. Düzgünes, K.R. Yamamoto, J. Biol. Chem. 265 (1990) 10189–10192.

[17] X. Gao, L. Huang, Biochemistry 35 (1996) 1027–1036.

[18] J.G. Smith, R.L. Walzem, J.B. German, Biochim. Biophys. Acta 1154 (1993) 327–340.

[19] N.J. Zuidam, Y. Barenholz, Biochim. Biophys. Acta 1329 (1997) 211–222.

[20] S. Levy, D. Avni, N. Aariharan, R.P. Perry, O. Meyuhas, Proc. Natl. Acad. Sci. U.S.A. 88 (1991) 3319–3323.

[21] Y. Barenholz, S. Amselem, Liposome preparation and related techniques, in: G. Gregoriadis (Ed.), Liposome Technology, vol. 1, 2nd ed., CRC Press, Boca Raton, FL, 1993, pp. 527–616.

[22] T. Maniatis, E.F. Fritsch, J. Sambrook, Molecular Cloning, A Laboratory Manual, Cold Spring Harbor Laboratory, Cold Spring Harbor, NY, 1982.

[23] B. Sternberg, J. Liposome Res. 6 (1996) 515–533.

[24] R. Pal, W.A. Petri, V. Ben-Yashar, R.R. Wagner, Y. Barenholz, Biochemistry 24 (1985) 573–581.

[25] V. Borenstain, Y. Barenholz, Chem. Phys. Lipids 64 (1993) 117–127.

[26] M.S. Fernández, P. Fromherz, J. Phys. Chem. 81 (1977) 1755–1761.

[27] M.S. Fernández, Biochim. Biophys. Acta 646 (1981) 23–26.

[28] R. Pal, W.A. Petri, Y. Barenholz, R.R. Wagner, Biochim. Biophys. Acta 729 (1983) 185–192.

[29] S.J. Eastman, C. Siegel, J. Tousignant, A.E. Smith, S.H. Cheng, R.K. Scheule, Biochim. Biophys. Acta 1325 (1997) 41–62.

[30] J.O. Rädler, I. Koltover, T. Salditt, C.R. Safinya, Science 275 (1997) 810–814.

[31] J. Gustaffson, G. Arvidson, G. Karlsson, M. Almgren, Biochim. Biophys. Acta 1235 (1995) 305–312.

[32] H. Gershon, R. Ghirlando, S.B. Guttman, A. Minsky, Biochemistry 32 (1993) 7143–7151.

[33] J. Langowski, W. Kermer, U. Kapp, Methods Enzymol. 211 (1992) 430–448.

[34] G. Cevc, Chem. Phys. Lipids 64 (1993) 163–186.

[35] E. Kalmanzon, E. Zlotkin, Y. Barenholz, Tenside Surfactants Detergents 26 (1989) 338–342.
[36] D. Hirsch-Lerner, Y. Barenholz, Biochim. Biophys. Acta, in press.
[37] N.J. Zuidam, D. Hirsch-Lerner, Y. Barenholz, Proceedings of Liposome Advances: Progress in Drug and Vaccine Delivery, London, December 16–20, 1996, p. 28.
[38] S.M. Gruner, Proc. Natl. Acad. Sci. U.S.A. 82 (1985) 3665–3669.
[39] D.C. Litzinger, L. Huang, Biochim. Biophys. Acta 1113 (1992) 201–227.
[40] F.L. Sorgi, L. Huang, Proc. Int. Symp. Control. Rel. Bioact. Mater. 22, Proceedings of a Symposium of the Controlled Release Society in Seattle, 1995, pp. 460–461.
[41] D.D. Lasic, H. Strey, M.C.A. Stuart, R. Podgornick, P.M. Fredrick, J. Am. Chem. Soc. 119 (1997) 832–833.
[42] N. Dan, Biochim. Biophys. Acta, submitted, 1997.
[43] R.B. Gennis, Biomembranes-Molecular Structure and Function, Springer, Berlin, 1989.
[44] J.N. Israelachvili, Intermolecular and Surface Forces, 2nd ed., Academic Press, London, 1991.
[45] S. May, A. Ben-Shaul, Biophys. J., submitted, 1997.
[46] N. Ostrovsky, Chem. Phys. Lipids 64 (1993) 45–56.